J Mater Sci (2009) 44:591–600
DOI 10.1007/s10853-008-3069-0

Precipitation of complex carbonitrides in a Nb–Ti microalloyed plate steel

H. R. Wang · W. Wang

Received: 12 November 2007 / Accepted: 17 October 2008 / Published online: 10 November 2008

Abstract Complex carbonitrides precipitated in base metal and heat-affected zone (HAZ) in Nb–Ti hot-rolled microalloyed steel plates have been identified to be Ti-rich (Nb, Ti)(C, N). As the reheating temperature is decreased from 1,200 to 1,150 °C, the average particle size in base metal is decreased from 40 to 20 nm. The morphology of complex carbonitrides in the HAZ, however, is transformed from cuboidal to rectangle shape with length of over 500 nm. Reheating at low temperature 1,150 °C may improve the toughness of HAZ by reducing the austenite size at large heat input welding.

Introduction

It is well established that the microalloying elements, such as Nb, Ti, and V, independently or in combination, can trigger the grain refinement through the precipitation of carbides, nitrides, and carbonitrides in austenite during reheating or hot rolling. In particular, titanium is most commonly used to control austenite grain size by the formation of titanium nitride with high thermal stability during welding, especially after high heat inputs. Jun et al. [1] observed three types, i.e., dendritic, semi-dendritic, and rod-like, Nb-rich (Nb, Ti)(C, N) complex carbonitrides in a continuously cast Nb–Ti bearing steel. Hong et al. [2] studied the effect of Ti addition on strain-induced precipitation kinetics of NbC in Nb-microalloyed steels. Poths et al. [3] found that the core of carbonitrides is mainly based on titanium nitride, which is decorated by a layer or cap of niobium carbide. Similar results were also observed by Craven et al. [4], who made a detailed study of complex precipitates in Al-killed Nb–Ti HSLA steels. They found that the core of carbonitrides is also based on TiN but with a spherical, cubic, or cruciform shape. In addition, the precipitation of carbonitrides in Nb–V and Ti–V [5] as well as Nb–Ti–V [6, 7] microalloyed steels was also studied by several authors.

Besides, the thermodynamic calculations on Nb–Ti [8–10] and Nb–Ti–V [11] steels were also performed. For example, Zou and Kirkaldy [8] carried out a thermodynamic study on Nb–Ti steels. Nearly at the same time, Okaguchi et al. [9] gave a computer model for predicting the carbonitride precipitation during hot working in Nb–Ti bearing steels. Recently, Liu [10] made a description of the phase equilibria between the austenite matrix and carbonitride precipitates thermodynamically. In addition, Inoue et al. [11] calculated the equilibria between the austenite and carbonitrides in Nb–Ti–V steels. The response of carbonitride particles to welding was studied by Suzuki et al. [12], and three types of behaviors were observed in Nb–V, Ti, and Nb–Ti microalloyed steels.

Very recently, many investigations are still concentrated on the precipitation in the Nb–Ti and Nb–Ti–V containing steels. Zeng et al. [13] made a quantitative description for the precipitation of carbonitrides in Nb–Ti microalloyed steels during hot deformation on the basis of thermodynamics and kinetics. Cao et al. [14] studied comparatively the precipitates in Nb–Mo and Nb–Ti containing steels from the viewpoints of the morphology, size distribution, composition, and crystal structure. They found that the fine and uniformly distributed MC-type carbides in Nb–Mo containing steels are superior to coarse and sparsely distributed carbonitrides in Nb–Ti containing steels in terms of

H. R. Wang (✉) · W. Wang
Metallurgical Process Department, Baosteel Research Institute, 889 Fujin Road, Shanghai 201900, People's Republic of China
e-mail: wanghr@baosteel.com

increasing yield strength. Similar study was also performed by Davis et al. [15], who studied the inhomogeneous precipitate distributions from different positions in Nb–Ti–V containing steels with varying Nb levels. In the area of weld thermal simulation, Bang et al. [16] gave an investigation of the effects of nitrogen content and weld cooling time on the toughness of heat-affected zone (HAZ) in a Ti-containing steel. And an optimal condition, ranging from 60 to 100 s for welding cooling time and 0.006% for nitrogen content, was obtained for high toughness of HAZ at −20 °C. This indicates that, although there have been some previous investigations, the precipitation behavior in Nb–Ti steels has not been well understood. Thus, the purpose of this study is to identify the strain-induced precipitates in matrix and HAZ and to examine the effect of reheat temperature and weld thermal cycle on the precipitation behavior in Nb–Ti bearing HSLA steels.

Experimental

The chemical composition of the Nb–Ti microalloyed plate steel used in this study is given in Table 1. The steel ingots, 100 kg each, were prepared in a vacuum induction furnace. Both ingots were homogenized at 1,200 and 1,150 °C for 2 h, and hot rolled to about 40-mm thick steel plate with total deformation of ~80%. Specimens of 11 × 11 × 55 mm for weld simulations were machined from the steel plates at the 1/4 thickness position. Weld thermal cycle simulations were conducted using Gleeble 3800 thermo-mechanical simulator. The specimens were heated to the peak temperature of 1,350 °C at a rate of 300 °C/s and held at the peak temperature for 1 s prior to the accelerated cooling. The cooling times from 800 to 500 °C ($\Delta t_{8/5}$) were 30.28, 60.55, and 151.38 s for both steel plates corresponding to heat inputs of 100, 200, and 500 kJ/cm, respectively. Typical weld thermal cycle time–temperature curves could be obtained elsewhere [17].The size and morphology of the precipitates extracted from the specimens in base metal and HAZ, were examined in a JEM 2100F field emission transmission electron microscopy (TEM) with an attachment of energy dispersive spectrum (EDS). The schematic diagrams for heat treatment and hot rolling for experimental steel plates are shown in Fig. 1. Also included in Fig. 1 is the typical weld thermal cycles at different heat inputs. Standard Charpy V-notch impact tests for HAZ at the required temperature of −20 °C were conducted using an SCL112-450J machine. In each case of welding heat input, the samples were tested for three times to obtain the reliable impact energy at −20 °C. Optical microscopy (OM) observations were performed in the Leica equipment, and the samples for OM were prepared by using the standard metallographic techniques. About 4% Nital etching solution is employed to reveal the microstructures of HAZ.

Table 1 Chemical composition of the steel examined in this study (wt.%)

C	Si	Mn	Al	Nb	Ti	N	Bal.
0.066	0.29	1.32	0.033	0.014	0.017	0.0063	Fe

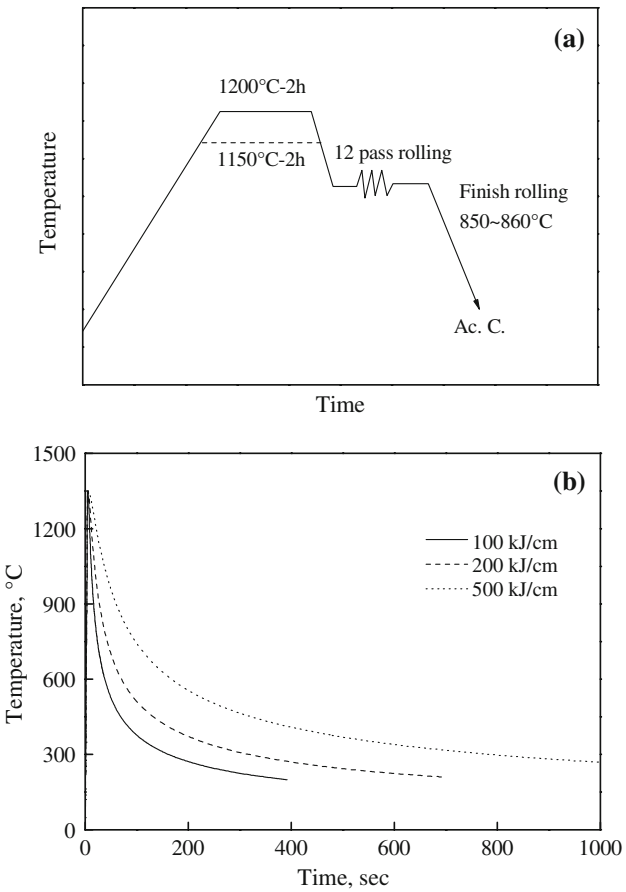

Fig. 1 Schematic diagrams showing the **a** reheating and hot-rolling processes, and **b** typical weld thermal cycles for Nb–Ti bearing steels

Results

Precipitation in the base metal

Figure 2 shows the TEM images for carbon replicas extracted from the base metal of specimens reheated at 1,200 °C for 2 h. It is observed in Fig. 2a that some cuboidal or rectangle particles are precipitated in the matrix, ranging from several to tens of nanometers. To identify the characters of these precipitates, EDS analysis was carried out and the results are shown in Fig. 2b. From

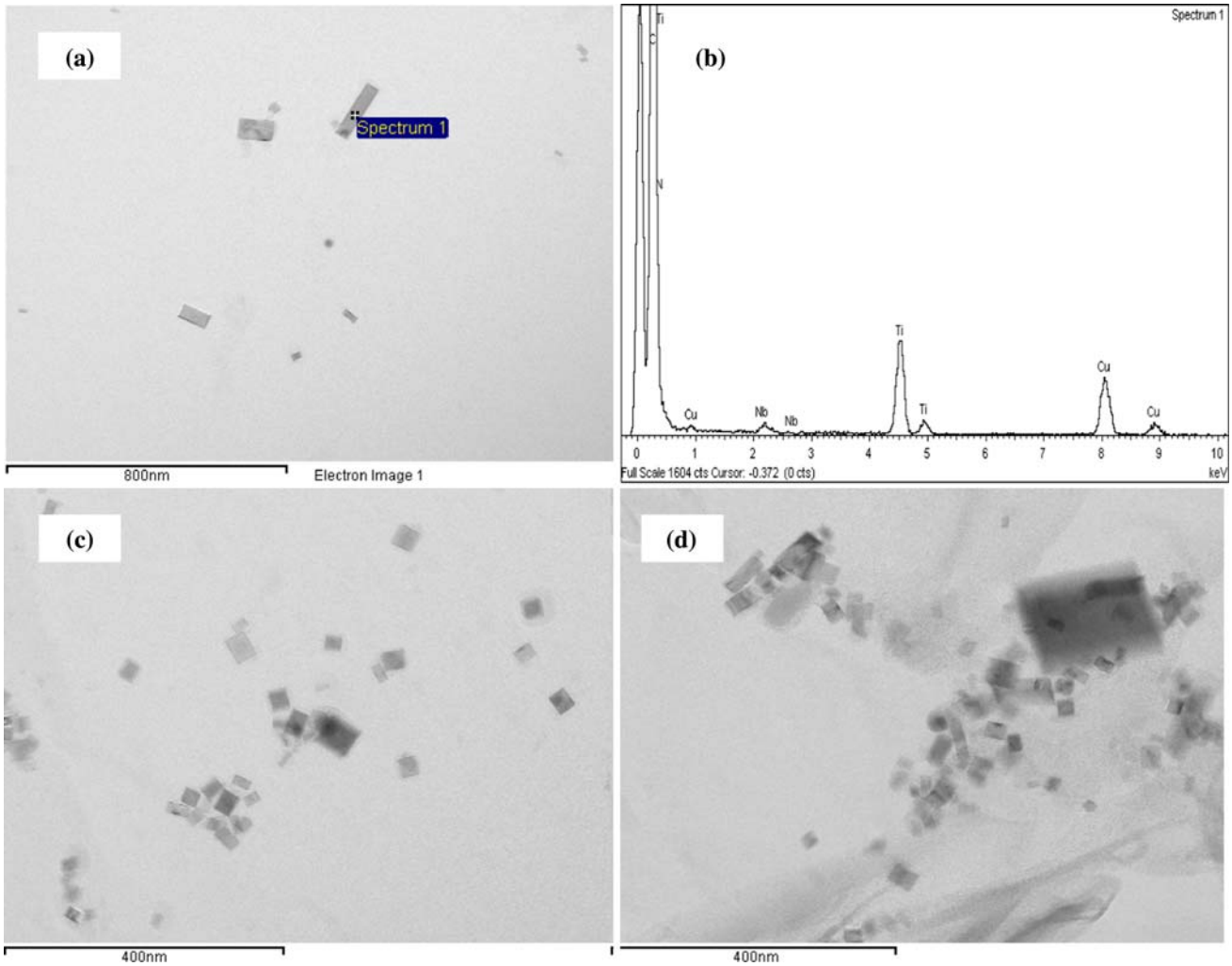

Fig. 2 TEM images and EDS analysis for carbon replicas extracted from the base metal of specimens reheated at 1,200 °C for 2 h

the EDS result it is evident that these precipitate particles are Ti-rich (Nb, Ti)(C, N) carbonitrides. The Cu peaks arise from the copper mesh supporting the carbon replica. Due to the limitations of EDS only semi-quantitative information on the amount of microalloying elements is obtained. It can be observed in Fig. 2c that the precipitates are uniformly distributed in the matrix, with a mean size of around 40 nm. On the other hand, a small amount of large particles are also appeared, as shown in Fig. 2d. A large particle of $\sim$150 nm occurred in the base metal, which is expected to be formed during ingot casting. In certain areas, the precipitates are heterogeneously distributed and exhibit grouping or clustering tendency, as described by Tian et al. [18], which is partially attributed to the strain-induced precipitation of complex carbonitrides.

Similar results are obtained for the specimens reheated at 1,150 °C for 2 h. Figure 3 displays the TEM micrographs for carbon replicas extracted from the samples reheated at 1,150 °C. It is obvious that the uniformly distributed particles are precipitated in the base metal, having an average size of about 20 nm, smaller than those obtained in the base metal of specimens reheated at 1,200 °C. This may be ascribed to the lower reheat temperature, which gives rise to the sluggish growth kinetics of precipitates during hot rolling. EDS analysis for precipitates further confirmed that these small particles are Ti-rich (Nb, Ti)(C, N) complex carbonitrides, as depicted in Fig. 3b. As a whole, the precipitates are homogeneously distributed in the matrix (Fig. 3c). In some areas, however, a few large precipitates are observed, typically shown in Fig. 3d with a size of $\sim 100 \times 100 \times 150$ nm. The Cu peaks also result from the copper mesh. EDS analysis confirmed that this large particle is also a Ti-enriched (Nb, Ti)(C, N) complex carbonitrides.

Precipitation in the HAZ

After weld thermal cycle simulation, the precipitation behavior in the HAZ is quite different. This is due to the fact that the precipitate in the HAZ undergoes a dissolution

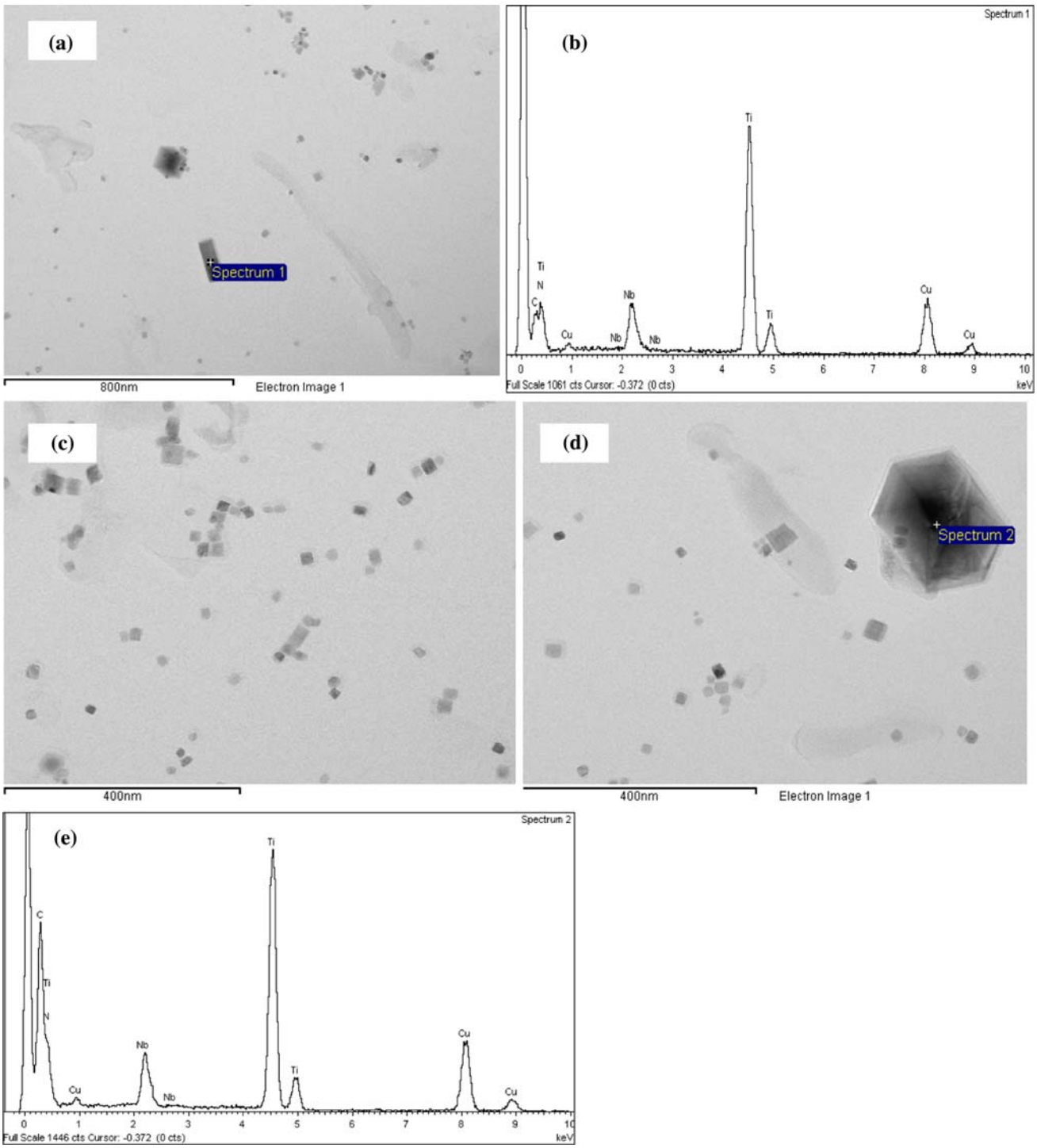

Fig. 3 TEM images and EDS analysis for carbon replicas extracted from the base metal of specimens reheated at 1,150 °C for 2 h

and reprecipitation process, as discussed by Suzuki et al. [12]. Figure 4 shows the TEM images for carbon replicas from the HAZ of specimens reheated at 1,200 °C. It is apparent that the average particle size is increased after weld simulation, typically in the range of 150–200 nm. Corresponding EDS result confirmed the precipitates to be again Ti-rich (Nb, Ti)(C, N) carbonitrides, as shown in Fig. 4b. However, in certain areas shown in Fig. 4c large cuboidal precipitates of hundreds of nanometers are clearly observed. It is noteworthy that the ratio of Nb to Ti, i.e., relative amounts of Nb and Ti in the base metal and HAZ, is remarkably different. In the base metal of Nb–Ti steels, the Nb/Ti ratio is around 1:3 while in the HAZ the Nb/Ti ratio reaches 1:5. This behavior implies that the

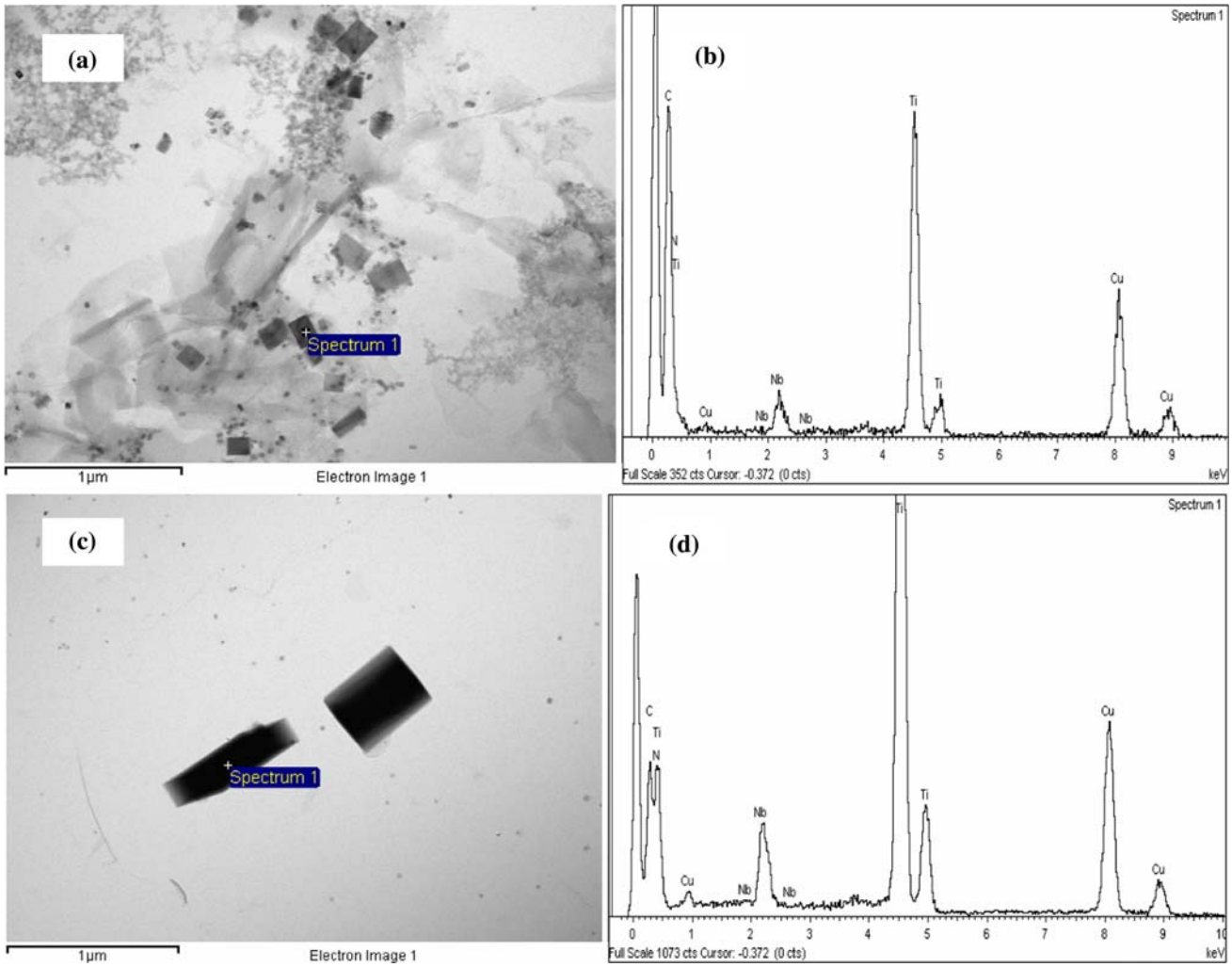

Fig. 4 TEM images and EDS analysis for carbon replicas extracted from the HAZ of specimens reheated at 1,200 °C for 2 h

precipitates in the HAZ become more Ti-rich than those in the base metal.

The precipitation behavior in the HAZ of specimens reheated at 1,150 °C, however, is different from those in the HAZ of samples reheated at 1,200 °C. The TEM micrographs and EDS results are shown in Fig. 5. It is of considerable interest to notice that a large amount of rectangle or rod-like precipitates appeared in the HAZ, some of which are located at grain boundaries. All EDS results identified these precipitates to be Ti-rich (Nb, Ti)(C, N) carbonitrides. In Fig. 5c it is evident that these precipitates are distributed heterogeneously and has the tendency of grouping and clustering. Through careful observation we can see that small caps are formed (circled by dashed lines) at the top of rectangle precipitates, which are also Ti-rich (Nb, Ti)(C, N) carbonitrides, as evidenced later. A typical micrograph of clusters of rectangle precipitates are shown in Fig. 5e with the largest edge length of over 500 nm.

Discussion

Precipitate composition and evolution in the base metal

Figure 6a shows the Nb and Ti content in austenite matrix in the temperature range of interest in light of our previous study [19]. Also included in Fig. 6a is the equilibrium volume fraction of precipitates in Nb–Ti bearing steels. Obviously, the amount of Nb and Ti in solution increases with increasing temperature while the volume fraction of precipitates decreases. Shown in Fig. 6b is the variation in equilibrium chemical composition of complex carbonitrides in Nb–Ti steels on the assumption that the carbonitrides can be written in the form of $(Nb_xTi_y)(C_zN_{1-z})$, where $x + y = 1$. The values of x, y, and z are dependent on the steel composition and temperature. Of special interest in Fig. 6b is that in the whole temperature range 800–1,300 °C the precipitates in our case are Ti-rich $(Nb_xTi_y)(C_zN_{1-z})$ complex carbonitrides, and accord well

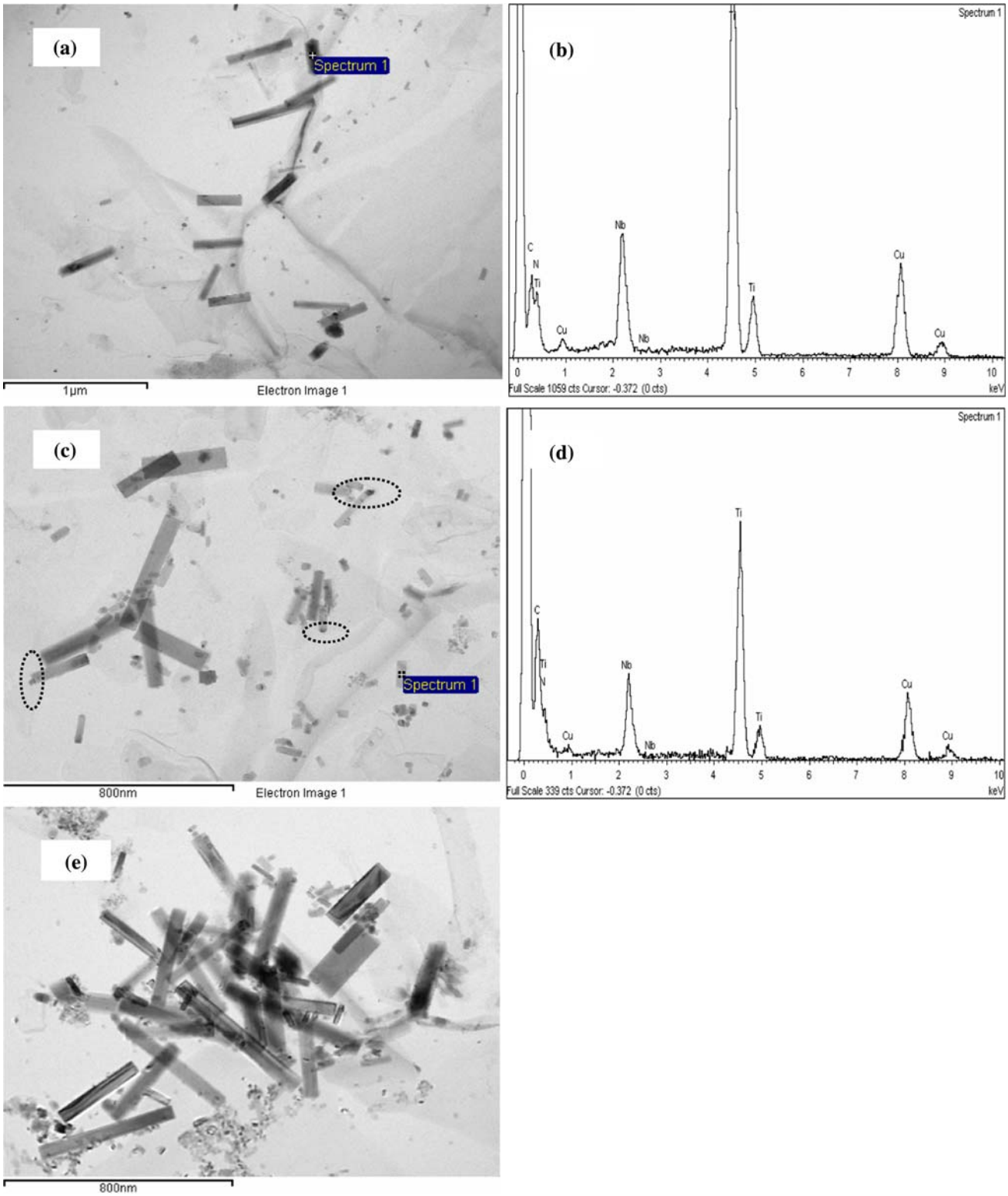

Fig. 5 TEM images and EDS analysis for carbon replicas extracted from the HAZ of specimens reheated at 1,150 °C for 2 h

with experimental observations. At 1,200 and 1,150 °C, the compositions of carbonitride are $(Nb_{0.12}Ti_{0.88})(C_{0.25}N_{0.75})$ and $(Nb_{0.15}Ti_{0.85})(C_{0.26}N_{0.74})$. If we take the steel chemistry of Jun et al. [1] as the initial inputs, we can obtain the composition of complex carbonitrides as $(Nb_{0.63}Ti_{0.37})(C_{0.58}N_{0.42})$ at 800 °C and $(Nb_{0.39}Ti_{0.61})(C_{0.44}N_{0.56})$ at 1,200 °C. The calculated results are also in good agreement with the experiments, i.e., Nb-rich (Nb, Ti)(C, N) at the

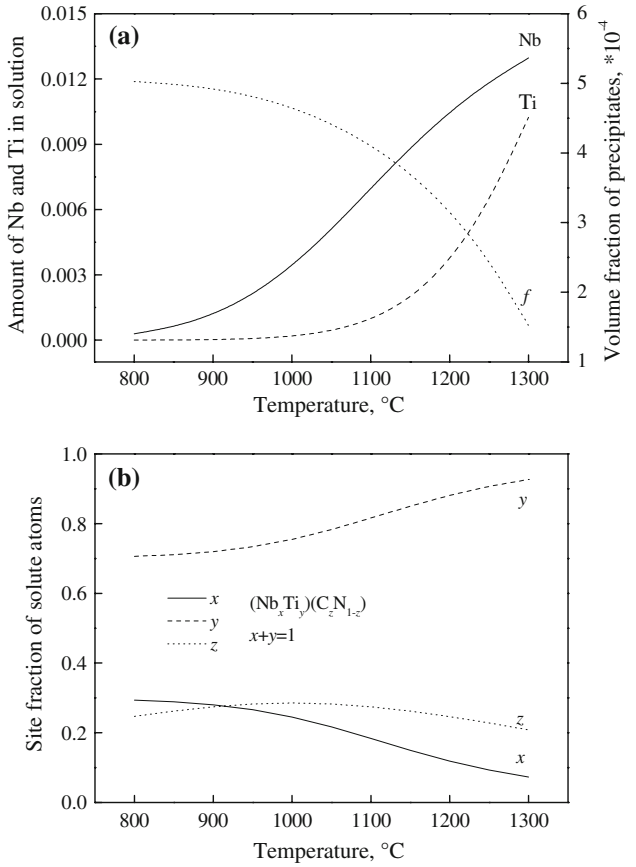

Fig. 6 **a** Solubility of Nb and Ti and equilibrium volume fraction of precipitates, and **b** compositional variation of complex carbonitrides in Nb–Ti bearing steels in a temperature range of interest

lower temperatures and Ti-rich (Nb, Ti)(C, N) at higher temperatures. Alternatively, the presence of Nb-rich (Nb, Ti)(C, N) complex carbonitrides is attributed to the high Nb content (0.056 wt.%) in their steel composition.

As mentioned before, non-equilibrium precipitates with dendritic, semi-dendritic, and rod-like morphologies were observed by Jun et al. [1] during continuous casting of Nb–Ti bearing steels. It is of interest to note that such precipitates disappeared during reheating process in the temperature range of 1,100–1,400 °C, followed by the formation of cubic shape precipitates [6]. It is well known that the evolution of precipitates is closely related to the dissolution temperature. In general, the dissolution temperature of complex carbonitrides is lower than that of carbides and/or nitrides. In Nb–Ti bearing steels, the TiN is the most stable phase among the four phases, i.e., NbC, NbN, TiC, and TiN. Based on the chemistry of Jun et al. [1], the contents of Ti and N are 0.018 and 0.004, in combination with the solubility product of TiN, i.e., $\log_{10}[\mathrm{Ti}][\mathrm{N}] = 4.94–14{,}400/T$, we can obtain the equilibrium dissolution temperature of TiN as 1,312 °C. It was, however, observed that the complex precipitates in slabs almost completely disappeared at the lower temperature of 1,100 °C. This behavior means that the complex carbonitrides are more prone to be dissolved than pure TiN nitrides.

Considering the fact that with increasing temperature, the chemical composition of complex carbonitrides becomes more titanium and nitrogen rich, as shown in Fig. 6. It is believed that the dissolution temperature of precipitates can be approximately estimated by that of pure TiN nitrides because the composition of precipitates at high temperatures is close to pure TiN nitrides. According to the solubility product of TiN given above, the equilibrium solution temperature of precipitates in our case is about 1,343 °C. This suggests that only partial dissolution of precipitates occurs when reheated at 1,200 and 1,150 °C. These undissolved Ti-rich (Nb, Ti)(C, N) precipitates are beneficial to the retardation of austenite grain at high temperature. It is obvious that reheating at 1,200 °C results in finer particle size and lower particle volume fraction than those at 1,150 °C. In other words, prior to hot rolling, the mean particle size in steel plate reheated at 1,200 °C is smaller than that reheated at 1,150 °C. During hot rolling, however, these undissolved Ti-rich (Nb, Ti)(C, N) carbonitrides may serve as nucleation sites for strain-induced newly formed precipitates. Alternatively, the Ostwald ripening of the undissolved precipitates may also occur simultaneously. Irrespective of the smaller initial particle size in steel plate reheated at 1,200 °C, the rate of growth of precipitates is faster than that reheated at 1,150 °C. This is because the rate of deformation is the same at each hot-rolling pass for two Nb–Ti steel plates, and thus, the rolling temperature of steel plate reheated at 1,150 °C at the same pass is lower than that reheated at 1,200 °C. As a result, the sluggish coarsening kinetics in the specimens reheated at 1,150 °C causes smaller mean particle size than that of carbonitrides in base metal of specimens reheated at 1,200 °C during multipass hot rolling. If the steel plates reheated at 1,200 and 1,150 °C are designated as A and B, respectively, then the precipitates evolution in steel ingot including particle volume fraction and mean particle size on heat treatment and hot rolling is schematically shown in Fig. 7.

It is well known that defects such as grain boundaries, interfaces, dislocations, and vacancies are favorable for the nucleation of precipitates. As discussed by Tian et al. [18], the particles tend to be present in clusters if they form on subgrain boundaries, tangled dislocation lines, and/or at the corners of grains. However, in the course of a welding thermal cycle, the subgrain boundaries and dislocations are almost completely absent due to very high temperature (e.g. 1,350 °C). It is thus the undissolved precipitates which are responsible for the grain refinement in the coarse-grained HAZ. In the subsequent cooling, these pre-existing precipitates may act as nucleation sites or

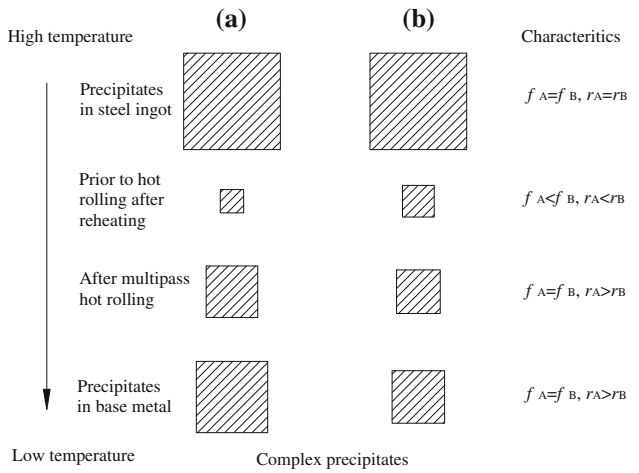

Fig. 7 Schematic illustration exhibiting the precipitates evolution in steel ingot during heat treatment and hot rolling

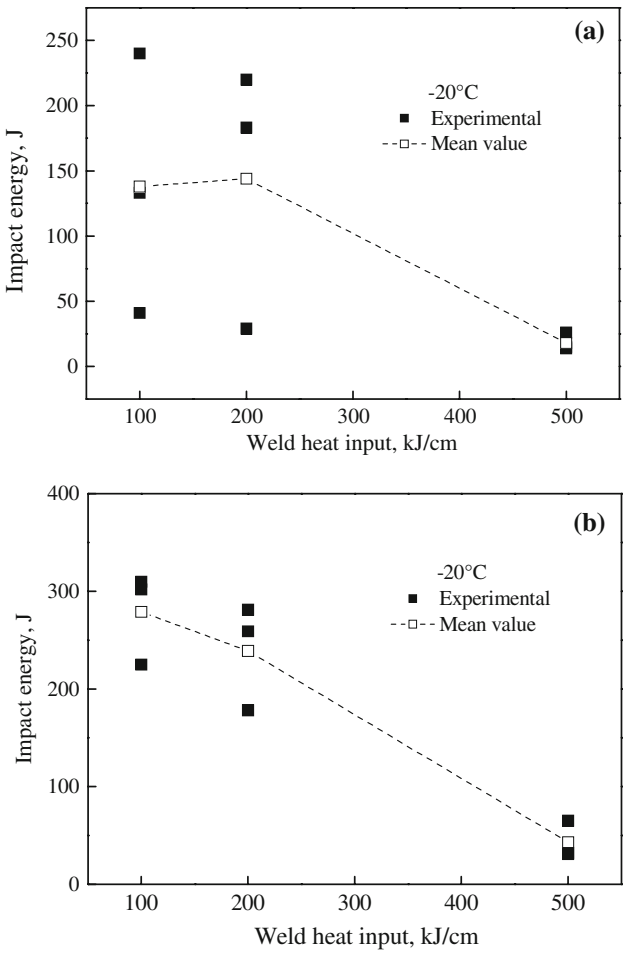

Fig. 8 Charpy V-notch impact energy of the HAZ at −20 °C for weld simulated specimens reheated at **a** 1,200 °C and **b** 1,150 °C as a function of welding heat input

continue to grow. As a consequence, the grouping tends to take place and to be further intensified by a weld thermo-cycle, particularly in Fig. 5c and e. The rectangle precipitates in Fig. 5 are suggested to occur along grain boundaries, and they are more effective than cuboidal ones to restrict the prior austenite grain size. The initial microstructural differences in both steel plates are thought to be eliminated during welding. Precipitates in the HAZ undergo a rapid dissolution and reprecipitation process after the high heat input welding. It is believed that the austenite grain size does not influence the precipitation kinetics of complex carbonitrides, as reported by Dutta et al. [20]. A consequence of this is that the precipitation kinetics in the HAZ during cooling leg of weld thermal cycle is mostly affected by the undissolved precipitates during rapid heating process.

Impact toughness, microstructure, and precipitate evolution in the HAZ

Figure 8 shows the V-notch absorbed impact energy of the HAZ at −20 °C for specimens at 1,200 and 1,150 °C as a function of welding heat input. As expected, in both cases the impact toughness of the HAZ at −20 °C decreases with increasing the welding heat input, which decreases from 138 J at 100 kJ/cm to 18 J at 500 kJ/cm for the specimens at 1,200 °C. As for the specimens at 1,150 °C, the impact energy depresses from 279 to 17 J as the heat input increases from 100 to 500 kJ/cm. The impact toughness of the HAZ depends largely on the microstructural constituent and grain size. In the circumstance of the same constituents, the coarse-grained region of HAZ is susceptible to the grain size. Obviously, the finer the prior austenite grain size the better the impact toughness. It is generally known that the prior austenite grain size at high temperatures is in association with the particle volume fraction and mean particle size. It is shown that the grain size in coarse-grained HAZ changes with the heat input according to the relationship, i.e., $d = k_1 k_2 (r/f)$, where k_1 is 4/3 and k_2 is related to heat input and assumed to be 1/2 [18]. Thus, the grain size of coarse-grained HAZ is determined by r/f. In view of the same particle volume fraction in both cases when the identical weld thermal cycle is applied. From the aforementioned, it is reasonable to conclude that the mean particle size play a significant role for impact toughness of the HAZ. From Figs. 2 and 3, we know that the mean particle size in the specimens reheated at 1,200 °C is coarser than that at 1,150 °C, and therefore, the prior austenite grain in steel plate at 1,150 °C is finer than that at 1,200 °C, which gives rise to better impact toughness.

Figure 9 shows the light micrographs from the HAZ of specimens after high heat input welding thermal cycle of 200 kJ/cm. It is clearly observed that the microstructures of specimens reheated at 1,200 °C are much coarser than

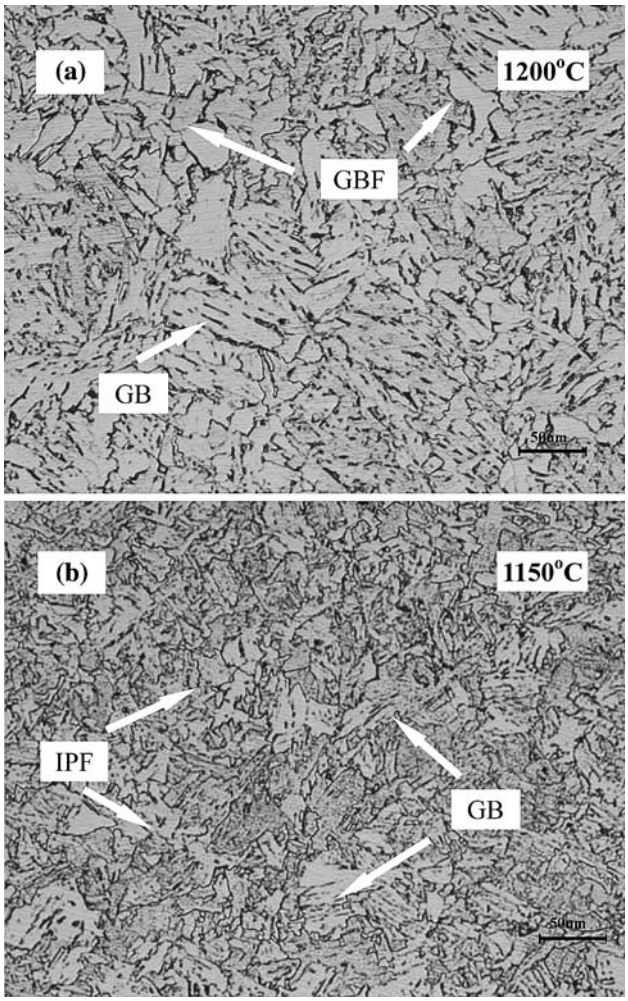

Fig. 9 Optical micrographs showing the microstructures of HAZ after high heat input welding of 200 kJ/cm

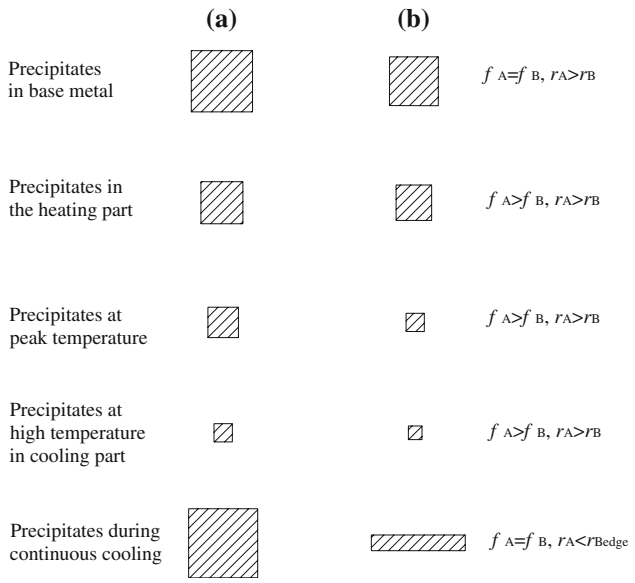

Fig. 10 Schematic illustration exhibiting the precipitates evolution in base metal during weld thermal cycle

those reheated at 1,150 °C. The microstructure of the HAZ at 1,200 °C mainly consists of coarse grain boundary ferrite (GBF) and granular bainite (GB). However, in the HAZ reheated at 1,150 °C the microstructure is mainly composed of fine irregular polygonal ferrite (IPF) and granular ferrite. It is, thus, deduced that the prior austenite grains at high temperature are finer in the specimens reheated at 1,150 °C than those reheated at 1,200 °C owing to the more dispersed distribution of precipitates with smaller mean particle size in the former. In the subsequent cooling process, the finer microstructures are readily obtained and the impact toughness of HAZ is greatly improved. The ferrite formation is attributed to the long cooling time $\Delta t_{8/5}$ caused by the large heat input welding. Besides, the formation of coarse grain boundary ferrite in Fig. 9a is related to the large prior austenite grain at 1,200 °C. From the viewpoint of practice, reheating at relatively lower temperature is favorable for the reduction of energy consumption and product cost.

The dissolution of Ti-rich (Nb, Ti)(C, N) complex precipitates on rapid heating involves the decomposition of precipitates and the diffusion of different species such as Nb, Ti, C, N etc., in the rapid heating stage, the rate of decomposition of precipitates is fast while the diffusion rates of solute atoms, particularly substitutional elements, are relatively slow. These solute atoms rejected from the complex precipitates are concentrated in the surrounding matrix, increasing the solubility product of TiN etc., in local regions and retarding the further dissolution. As a result, in the heating part of thermal cycle, an equilibria of dissolution is not reached and no reprecipitation takes place. Furthermore, the dissolution may occur in the cooling part at high temperatures. The morphology of rectangle precipitates in the HAZ of steel plate reheated at 1,150 °C is probably ascribed to the preferential nucleation and growth along the austenite grain boundaries. The precipitates evolution in base metal during weld thermal cycle in this study are schematically depicted in Fig. 10. Further investigations are required to clarify the mechanism of the formation of such complex precipitates.

Conclusions

To summarize, the precipitates in Nb–Ti bearing steels are identified as Ti-rich (Nb, Ti)(C, N) carbonitrides both in base metal and HAZ. As the reheating temperature is decreased from 1,200 to 1,150 °C, the particle size of cuboidal carbonitrides, which is uniformly distributed in the matrix in base metal, is reduced from 40 to 20 nm. For the Nb–Ti bearing steels reheated at 1,200 °C, the size of

complex carbonitrides in the HAZ is increased in comparison with those in the base metal, but the morphology remains basically unchanged. In contrast, for the Nb–Ti bearing steels reheated at 1,150 °C, the morphology of carbonitrides in the HAZ is transformed from cuboidal into rectangular shape with the largest edge length of exceeding 500 nm. When viewed from the practical production, reheating at relatively low temperature is beneficial to reduce the product cost.

Acknowledgements The authors would like to express their gratitude to Dr. Jiaqiang Gao at the Testing Centre of Baosteel Research Institute for his help in TEM operations and valuable discussions. The authors are also indebted to Engineer Guobin Song for performing the weld simulations in a Gleeble 3800 system.

References

1. Jun HJ, Kang KB, Park CG (2003) Scripta Mater 49:1081
2. Hong SG, Kang KB, Park CG (2002) Scripta Mater 46:163
3. Poths RM, Higginson RL, Palmiere EJ (2001) Scripta Mater 44:147
4. Craven AJ, He K, Garvie LAJ, Baker TN (2000) Acta Mater 48:3857
5. Pandit A, Murugaiyan A, Podder AS, Haldar A, Bhattacharjee D, Chandra S, Ray RK (2005) Scripta Mater 53:1309
6. Hong SG, Jun HJ, Kang KB, Park CG (2003) Scripta Mater 48:1201
7. Shanmugam S, Tanniru M, Misra RDK, Panda D, Jansto S (2005) Mater Sci Technol 21:883
8. Zou H, Kirkaldy JS (1992) Metall Trans A 23:651
9. Okaguchi S, Hashimoto T (1992) ISIJ Int 32:283
10. Liu ZK (2004) Scripta Mater 50:601
11. Inoue K, Ishikawa N, Ohnuma I, Ohtani H, Ishida K (2001) ISIJ Int 41:175
12. Suzuki S, Weatherly GC, Houghton DC (1987) Acta Mater 35:341
13. Zeng Y, Wang W (2008) J Mater Sci 43:874. doi:10.1007/s10853-007-2152-2
14. Cao JC, Yong QL, Liu QY, Sun XJ (2007) J Mater Sci 42:10080. doi:10.1007/s10853-007-2000-4
15. Davis CL, Strangwood M (2002) J Mater Sci 37:1083. doi:10.1023/A:1014342800399
16. Bang KS, Park C, Liu S (2006) J Mater Sci 41:5994. doi:10.1007/s10853-006-0498-5
17. Ashby MF, Easterling KE (1982) Acta Mater 30:1969
18. Tian DW, Karjalainen LP, Qian B, Chen X (1996) Metall Mater Trans A 27:4031
19. Wang W, Wang HR (2007) Mater Lett 61:2227
20. Dutta B, Sellars CM (1987) Mater Sci Technol 3:197